Tn-Seq Analysis Identifies Genes Important for *Yersinia pestis* Adherence during Primary Pneumonic Plague

Kara R. Eichelberger,[a] Victoria E. Sepúlveda,[a] John Ford,[b,c] Sara R. Selitsky,[b,c] Piotr A. Mieczkowski,[c] Joel S. Parker,[b,c] William E. Goldman[a]

[a]Department of Microbiology and Immunology, University of North Carolina at Chapel Hill, Chapel Hill, North Carolina, USA
[b]Lineberger Comprehensive Cancer Center, University of North Carolina, Chapel Hill, North Carolina, USA
[c]Department of Genetics, University of North Carolina, Chapel Hill, North Carolina, USA

ABSTRACT Following inhalation, *Yersinia pestis* rapidly colonizes the lung to establish infection during primary pneumonic plague. Although several adhesins have been identified in *Yersinia* spp., the factors mediating early *Y. pestis* adherence in the lung remain unknown. To identify genes important for *Y. pestis* adherence during primary pneumonic plague, we used transposon insertion sequencing (Tn-seq). Wild-type and capsule mutant (Δ*caf1*) *Y. pestis* transposon mutant libraries were serially passaged *in vivo* to enrich for nonadherent mutants in the lung using a mouse model of primary pneumonic plague. Sequencing of the passaged libraries revealed six mutants that were significantly enriched in both the wild-type and Δ*caf1 Y. pestis* backgrounds. The enriched mutants had insertions in genes that encode transcriptional regulators, chaperones, an endoribonuclease, and YPO3903, a hypothetical protein. Using single-strain infections and a transcriptional analysis, we identified a significant role for *YPO3903* in *Y. pestis* adherence in the lung and showed that YPO3903 regulated transcript levels of *psaA,* which encodes a fimbria previously implicated in *Y. pestis* adherence *in vitro*. Deletion of *psaA* had a minor effect on *Y. pestis* adherence in the lung, suggesting that YPO3903 regulates other adhesins in addition to *psaA*. By enriching for mutations in genes that regulate the expression or assembly of multiple genes or proteins, we obtained screen results indicating that there may be not just one dominant adhesin but rather several factors that contribute to early *Y. pestis* adherence during primary pneumonic plague.

IMPORTANCE Colonization of the lung by *Yersinia pestis* is a critical first step in establishing infection during primary pneumonic plague, a disease characterized by high lethality. However, the mechanisms by which *Y. pestis* adheres in the lung after inhalation remain elusive. Here, we used Tn-seq to identify *Y. pestis* genes important for adherence early during primary pneumonic plague. Our mutant enrichment strategy resulted in the identification of genes important for regulation and assembly of genes and proteins rather than adhesin genes themselves. These results reveal that there may be multiple *Y. pestis* adhesins or redundancy among adhesins. Identifying the adhesins regulated by the genes identified in our enrichment screen may reveal novel therapeutic targets for preventing *Y. pestis* adherence and the subsequent development of pneumonic plague.

KEYWORDS Tn-seq, *Yersinia pestis*, adherence, lung, plague, pneumonic plague

Inhalation of aerosolized droplets containing *Yersinia pestis* causes primary pneumonic plague, which is the most severe manifestation of plague. Once in the lung, *Y. pestis* establishes an anti-inflammatory environment that is permissive for rapid bacterial proliferation and leads to severe pulmonary inflammation (1, 2). Adherence to host cells is a critical first step during bacterial pathogenesis (3), and *Y. pestis* likely requires

adhesins to mediate attachment to airway cells for colonization of the lungs during primary pneumonic plague. The early events of primary pneumonic plague, particularly how *Y. pestis* adheres to cells in the small airways, are incompletely understood.

Two of the best-characterized adhesins in the genus *Yersinia* are YadA and invasin. *Yersinia pseudotuberculosis* and *Yersinia enterocolitica* utilize invasin and YadA to establish infection in the small intestine (4). Invasin binds β1 integrins on M cells, promoting internalization of the enteropathogenic *Yersinia* organisms (5). YadA has more diverse functions, including mediating attachment to epithelial cells and extracellular matrix proteins as well as promoting persistence of *Y. enterocolitica* in the Peyer's patches (6, 7). However, both YadA and invasin are absent in *Y. pestis*, due to an inactivating mutation in *yadA* and an insertional element in *inv* (8, 9). Therefore, other factors must be involved in facilitating *Y. pestis* adherence to host cells and colonization, particularly during primary pneumonic plague.

Using various cell culture infection models, four surface structures displayed by *Y. pestis* have been implicated in adherence: Pla, Ail, PsaA, and the F1 antigen. *Y. pestis pla* mutants are attenuated in primary pneumonic plague models of disease (10). The plasminogen activator protease, or Pla, has effects on adherence that are independent of its proteolytic activity (11). Pla binds laminin present in extracellular matrices and promotes invasion of HeLa cells (12, 13). Pla also facilitates *Y. pestis* type III secretion system (T3SS) translocation into alveolar macrophages (14, 15). However, *Y. pestis pla* mutants adhere to epithelial cell lines as well as wild-type *Y. pestis*, suggesting that Pla does not function as a dominant adhesin to the respiratory epithelium (16). In contrast, the attachment invasion locus, *ail*, has been proposed to encode a major adhesin in *Yersinia*. The *ail* gene is present and functional in all three human-pathogenic *Yersinia* and confers serum resistance (17–19). However, its effect on adherence varies among *Yersinia* species. Ail mediates host cell binding *in vitro* for *Y. enterocolitica*, but if introduced into nonpathogenic *Y. enterocolitica* species that do not contain the *ail* gene, it does not confer attachment or invasion (20). Deletion of *ail* in *Y. pseudotuberculosis* does not alter adhesion to host cells (18). In *Y. pestis*, adherence to epithelial cell lines *in vitro* is reduced only when *ail* is deleted in combination with other surface protein-encoding genes or when the bacteria are grown at an environmental temperature of 28°C (16, 21).

PsaA, or the pH 6 antigen, is a fimbria-like structure displayed on the cell surface of *Y. pestis* at 37°C and pH 6 (22). *Y. pestis* Δ*psaA* is less adherent to epithelial lines *in vitro* and also inhibits phagocytosis by macrophages when the bacteria are grown under inducing conditions of low pH and 37°C (23, 24). However, when *psaA* is deleted in a strain of *Y. pestis* lacking the F1 antigen, the bacteria are just as adherent as wild-type cells, suggesting the presence of other unknown adhesins (23). The F1 antigen, which is encoded by the *caf1* gene on the pMT1 plasmid, is a large polymer that forms an antiphagocytic capsule-like structure surrounding *Y. pestis* at 37°C (25–27). *Y. pestis* Δ*caf1* is more adherent to epithelial cell lines, and its deletion reveals the presence of large fimbria-like structures that extend from the cell surface (23, 28). Thus, expression of F1 antigen on the bacterial surface appears to mask or block the effect of other *Y. pestis* adhesins. It is unknown if Ail, PsaA, or the F1 antigen affects *Y. pestis* adherence in the lung during primary pneumonic plague.

Despite the identification and characterization of several proteins in the outer membrane of *Y. pestis*, no single factor has emerged as the dominant *Y. pestis* adhesin (21, 23, 29). Therefore, we used transposon insertion sequencing (Tn-seq) as an unbiased approach to identifying genes important for *Y. pestis* adherence during primary pneumonic plague. We performed *in vivo* serial enrichment using our mouse model of primary pneumonic plague to screen wild-type and Δ*caf1 Y. pestis* transposon mutant libraries for nonadherent mutants in the lung. Comparison of the identities of nonadherent mutants in *Y. pestis* wild-type and Δ*caf1* libraries indicated that there were six independent mutants significantly enriched in both strain backgrounds. These mutants had insertions in YPO3904 and *iscR*, which encode transcriptional regulators, in *tig* and *clpX*, which encode chaperones, in *rnc*, which encodes an endoribonuclease, and in

YPO3903, which encodes a hypothetical protein. We demonstrated a significant role for YPO3903 in *Y. pestis* adherence in the lung and in regulating transcript levels of *psaA*, the deletion of which had a minor effect on *Y. pestis* adherence in the lung. The enrichment of mutants that likely have altered gene expression and levels of multiple proteins suggests functional redundancy or the presence of multiple adhesins in *Y. pestis*.

RESULTS

***Yersinia pestis* genes important for adherence in the lung are unknown.** The earliest events of primary pneumonic plague, particularly how *Y. pestis* interacts with and adheres to cells in the small airways, are unknown. To characterize the initial adherence of *Y. pestis* in the lung, we used our mouse model of primary pneumonic plague to determine the proportion of adherent bacteria early after inoculation (2). Mice were inoculated intranasally with 1×10^4 CFU *Y. pestis* CO92 (wild type), and 2 h postinoculation (hpi), we performed a bronchoalveolar lavage of the lungs to remove any nonadherent *Y. pestis* and enumerated the proportion of *Y. pestis* that remained in the lung. We observed that approximately 75% of *Y. pestis* was adherent in the lung 2 h after inoculation (Fig. 1A, black bar).

The attachment invasion locus (Ail) has been implicated in adherence for *Y. entero-colitica* and *Y. pestis* to various cell lines, and a *Y. pestis ail* mutant exhibits reduced virulence following intranasal inoculation (16, 20, 30). Therefore, *ail* may play a role in adherence of *Y. pestis* in the lung early after inoculation. Additionally, it was recently shown that the *Y. pestis* type III secretion system (T3SS) needle tip protein, LcrV, binds the *N*-formylpeptide receptor (FPR1) on immune cells for delivery of T3SS effectors (31). It is therefore possible that T3SS binding to host FPR1 mediates *Y. pestis* adherence in the lung. To test the role of *ail* and the T3SS in *Y. pestis* adherence early during primary pneumonic plague, we inoculated mice intranasally with 1×10^4 CFU Δ*ail Y. pestis* or pCD1$^-$ *Y. pestis*, which lacks the plasmid encoding the T3SS needle apparatus and effectors (25). At 2 hpi, we performed a bronchoalveolar lavage and calculated the percentage of adherent *Y. pestis* for each strain. Approximately 75% of *Y. pestis* Δ*ail* and pCD1$^-$ was adherent in the lung, similar to the levels of adherence for wild-type *Y. pestis* (Fig. 1A). Total bacterial burdens in the lung for the three *Y. pestis* strains were also similar ($\sim 10^4$ CFU) at 2 hpi (Fig. 1B). Thus, despite the putative role of *ail* in *Y. pestis* adherence *in vitro* and LcrV binding to FPR1, our data suggest that these surface structures do not individually play a major role in mediating *Y. pestis* adherence in the lung early during primary pneumonic plague.

To identify genes important for *Y. pestis* adherence in the lung, we took an unbiased genetic approach using Tn-seq to screen comprehensive libraries of *Y. pestis* mutants for genes required for adherence. We predicted that mutants with transposon insertions in genes important for adherence in the lung would be enriched in the bronchoalveolar lavage fluid (BALF) collected from mice following intranasal inoculation with a *Y. pestis* transposon library. To enhance the enrichment of nonadherent mutants, we also created a comprehensive library of transposon insertional mutants in a *Y. pestis* Δ*caf1* strain in addition to the wild-type *Y. pestis* mutant library. The *caf1* gene encodes the F1 antigen, which forms a large capsule-like structure around *Y. pestis* at 37°C (26, 27). The presence of the F1 antigen on the surface of *Y. pestis* masks surface structures and adherence *in vitro* (23, 28). Therefore, the Δ*caf1* strain background may provide greater enrichment of nonadherent mutants without the masking effect of the F1 antigen.

A schematic depicting our enrichment strategy is shown in Fig. 1C. Briefly, we generated transposon input libraries of approximately 233,000 mutants for wild-type *Y. pestis* and approximately 208,000 mutants for *Y. pestis* Δ*caf1*. We then inoculated two groups of three mice each intranasally with either 1×10^6 CFU *Y. pestis* wild-type transposon mutants or 5×10^6 *Y. pestis* Δ*caf1* transposon mutants. Using a higher inoculum than our standard dose of 1×10^4 CFU ensured delivery of all transposon mutants to the lung. At the same time, a portion of each input library was inoculated
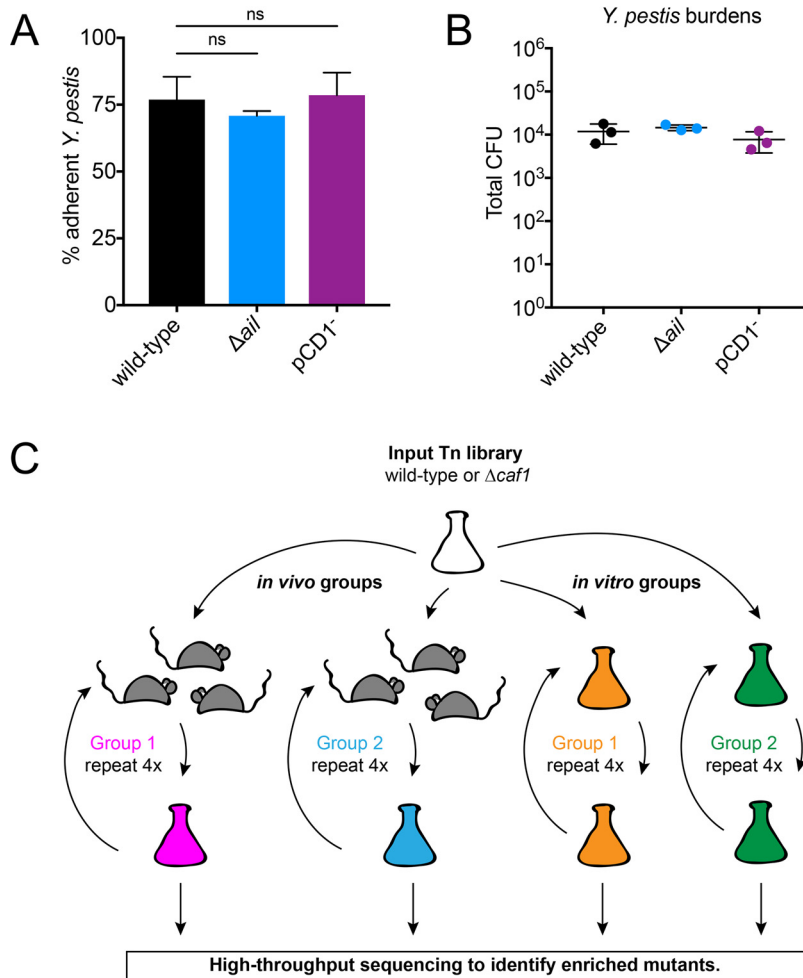
FIG 1 The *Yersinia pestis* genes important for adherence in the lung are unknown. Mice were inoculated intranasally with 1×10^4 CFU of the *Y. pestis* wild-type, Δ*ail*, or pCD1$^-$ strains, and bronchoalveolar lavage was performed at 2 hpi. CFU were enumerated in both the bronchoalveolar lavage fluid (BALF) and the lung. (A) Percent adherence was calculated for each strain by determining the proportion of *Y. pestis* in the lung compared to total CFU in both the BALF and the lung. Significance was determined by one-way ANOVA with Tukey's multiple correction. ns, not significant. (B) Total *Y. pestis* CFU enumerated in both the lung and the BALF. Data are representative of two independent experiments with 3 mice per group and are means and SD. (C) Schematic depicting the screen method for serial enrichment of nonadherent *Y. pestis* transposon mutants in both wild-type and Δ*caf1* strains. The input library was inoculated into 2 groups of 3 mice each or 2 *in vitro* culture flasks. At 2 hpi, bronchoalveolar lavage was performed on the mice to collect nonadherent *Y. pestis* mutants and a portion of the *in vitro* cultures were removed. These mutants were then used to inoculate new groups of mice and *in vitro* cultures, repeating the *in vivo* enrichment or *in vitro* controls, and this process was repeated for a total of four times to collect mutants for high-throughput sequencing to determine the identity of the enriched mutants.

into two replicate *in vitro* liquid cultures and grown with shaking at 37°C for *in vitro* growth controls. At 2 hpi, we collected BALF (containing *Y. pestis* mutants with adherence defects) from mice and a portion of each *in vitro* culture, and we plated these groups of mutants separately on selective media. Portions of these enriched mutants were then used to start liquid cultures for the next round of infection, keeping the two biological replicates for the *in vivo* and *in vitro* groups separate. This enrichment protocol was repeated three more times for a total number of four rounds of enrichment *in vivo* and *in vitro*. After each round of enrichment, genomic DNA was isolated from each group of *Y. pestis* mutants for sequencing of the transposon junctions to identify the enriched mutants.

Enrichment of less-adherent *Y. pestis* mutants after serial passaging of transposon libraries. During our Tn-seq screen, we calculated the proportion of adherent
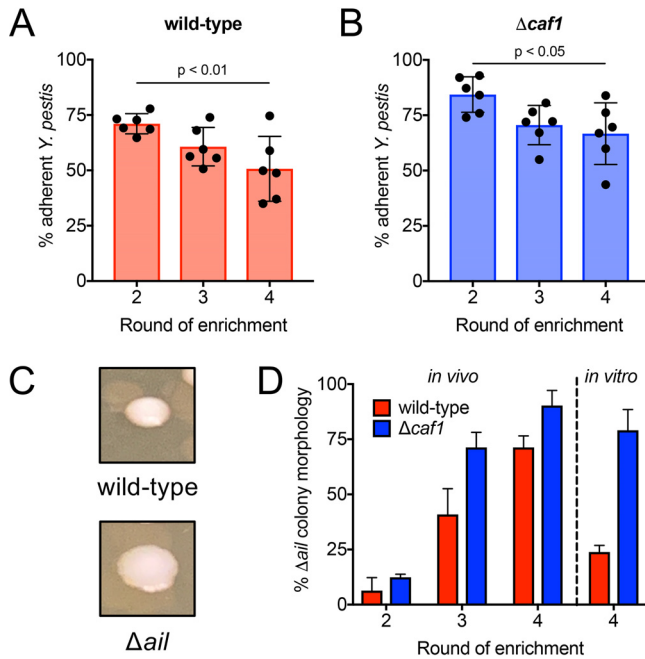
FIG 2 Enrichment of less-adherent *Y. pestis* mutants after serial passaging of transposon libraries. Mice were inoculated intranasally with 1×10^6 CFU of the *Y. pestis* wild-type transposon library or 5×10^6 CFU of the *Y. pestis* Δ*caf1* transposon library. Bronchoalveolar lavage was performed at 2 hpi, and CFU were enumerated in both the bronchoalveolar lavage fluid (BALF) and the lung. Percent adherence was calculated after two, three, and four rounds of *in vivo* enrichment by determining the proportion of *Y. pestis* transposon mutants in the lung compared to the total CFU of transposon mutants in both the BALF and the lung for wild-type (A) and Δ*caf1* (B) backgrounds. *P* values (A and B) were determined by one-way ANOVA with Tukey's multiple correction. (C) Colony morphology of a wild-type *Y. pestis* colony and a Δ*ail Y. pestis* colony, both in the pCD1⁻ strain background, grown at 26°C for 2 days on BHI agar. (D) The proportion of colonies in the BALF with a Δ*ail*-like morphology at two, three, and four rounds of enrichment *in vivo* and four rounds of enrichment *in vitro* for both wild-type (red bars) and Δ*caf1* libraries (blue bars). Data are means and SD.

bacteria after each round of enrichment *in vivo* for both *Y. pestis* wild-type and Δ*caf1* groups. The proportion of adherent wild-type *Y. pestis* insertional mutants in the lung decreased from 70% after two rounds of enrichment to ~60% by three rounds and ~50% by four rounds of enrichment (Fig. 2A). There was also a reduction in adherence for *Y. pestis* mutants in the Δ*caf1* background over four rounds of enrichment. There was approximately 85% adherence after two rounds of selection, and this decreased to ~70% adherence by three rounds and ~65% adherence by four rounds of enrichment (Fig. 2B). Together, these data indicate that there was significant enrichment of nonadherent mutants by serially passaging both the *Y. pestis* wild-type and Δ*caf1* transposon libraries through the lungs of mice. Additionally, the *Y. pestis* Δ*caf1* mutants were more adherent in the lung than the wild-type *Y. pestis* mutants at each round of selection, supporting previous observations that the F1 antigen masks *Y. pestis* adherence factors.

Correlated with the enrichment of nonadherent mutants after each *in vivo* passage of the transposon libraries, we also observed an increase in the proportion of an altered colony morphology for *Y. pestis* mutants collected in the BALF after each round of enrichment. The colonies were larger with a less-defined border compared to those of wild-type *Y. pestis*, which is indicative of an *ail* mutant (Fig. 2C) (21). For the nonadherent mutants in the wild-type background, approximately 6% of the colonies recovered in the BALF had the Δ*ail*-like colony morphology after two rounds of enrichment, which increased to 40% after three rounds and 70% after four rounds of enrichment (Fig. 2D, red bars). The enrichment for Δ*ail*-like mutants was stronger in the Δ*caf1* background, with 10% of nonadherent mutants having the Δ*ail*-like colony morphology after two rounds, increasing to 70% by three rounds and 90% by four rounds of

enrichment (Fig. 2D, blue bars). However, we also observed enrichment of Δail-like mutants in the in vitro control groups. After four rounds of enrichment in vitro, ~25% of the colonies in the wild-type in vitro controls had a Δail-like colony morphology, whereas nearly 75% of colonies in the Δcaf1 background had a Δail-like morphology (Fig. 2D). The in vitro enrichment suggests that Δail mutants may have a competitive growth advantage during the in vitro culture steps between inoculations that contributed to their enrichment during the in vivo screen, particularly in the Δcaf1 background. Due to the large proportion of Δail-like colonies (and thus likely mutants with transposon insertions in ail or genes that regulate ail) saturating the mutant pools after four rounds of enrichment, we performed high-throughput sequencing and subsequent analysis of the pools of nonadherent mutants collected after two and three rounds of selection.

Significant enrichment of mutations in genes involved in the regulation and assembly of macromolecules. We performed high-throughput sequencing using the MiSeq platform, sequencing the transposon junction to identify which mutants were enriched by the screen. We determined that approximately 25% of all TA sites in the genome contained a transposon insertion in the Δcaf1 input library, and 77% of annotated genes in the genome had at least one TA site disrupted. For the wild-type input library, approximately 37% of all TA sites in the genome contained a transposon insertion, and 83% of annotated genes had at least one TA site disrupted. Considering that about 10 to 15% of Y. pestis annotated genes were calculated to be essential (32), our input libraries had relatively good coverage of the genome. The number of unique reads for each gene was counted, upper quartile normalized, and $\log_2$ transformed. As there were two replicates for the in vivo and in vitro groups, we compared the similarity of the read count for each gene between the two replicates for each condition (Fig. S1). We observed a very strong correlation between the two replicates for each condition, with R^2 values of >0.99 for every condition except Δcaf1 2 rounds in vitro, which has an R^2 value of 0.94. This indicates a high level of reproducibility among the technical replicates in the screen. Thus, we averaged the replicate read count for each gene.

We then calculated the enrichment value for each gene. The enrichment value equals the fold change in the read count for a given gene after two and three rounds of enrichment relative to the read count for that gene in the input library. The goal of our screen was to identify significant enrichment of mutants with insertions in genes involved in Y. pestis adherence, so we focused on genes with enrichment values that were greater than two standard deviations (SD) from the mean after both two rounds and three rounds of enrichment in vivo. In the wild-type background, there were 51 genes that had enrichment values >2 SD from the mean (Fig. 3A, red dots). In the Δcaf1 background, there were 67 genes with enrichment values >2 SD from the mean (Fig. 3B, blue dots). For these significantly enriched mutants, we wanted to eliminate any that were enriched due to enhanced in vitro growth. To this end, we subtracted the in vitro enrichment values from the in vivo enrichment values for each significantly enriched gene (Fig. 3C and D). In the wild-type background, there were 18 genes that had greater enrichment values in vivo over in vitro (Fig. 3C, purple dots). In the Δcaf1 background, there were 34 genes with greater enrichment values in vivo relative to in vitro (Fig. 3D, green dots). The identity and enrichment values for each of these genes are listed in Table 1.

Of the 18 genes identified in the wild-type background and the 34 genes identified in the Δcaf1 background, six genes were shared between the two groups: clpX, tig, iscR, rnc, YPO3903, and YPO3904 (Fig. 3C). This small overlap in the identity of the significantly enriched mutants is reflective of comparing the enrichment values for every gene in the wild-type background relative to the enrichment value for the same gene in Δcaf1 background, where there was poor correlation at both two and three rounds of enrichment (Fig. S2). Because mutations in the six genes were significantly and independently enriched in both strain backgrounds, we hypothesized that these genes may play the greatest role in Y. pestis adherence in the lung. The six genes are all encoded on the Y. pestis chromosome, and none of these genes are annotated as
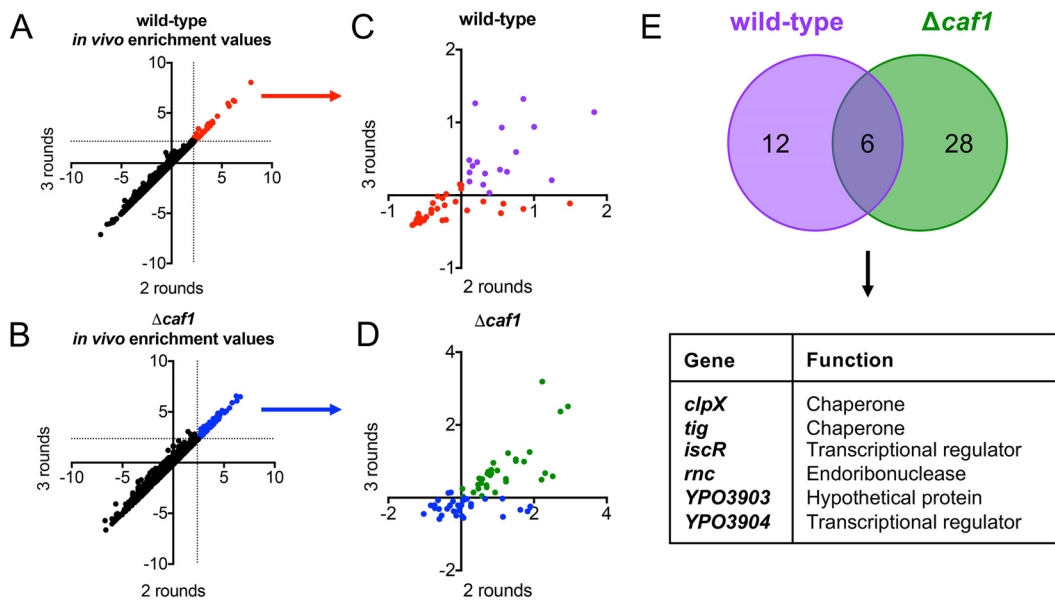
FIG 3 Significant enrichment of mutations in genes involved in the regulation and assembly of macromolecules. Libraries of the wild-type and Δ*caf1* transposon mutants were sequenced to identify the genes disrupted by the transposon insertion after two and three rounds of enrichment. Each gene was assigned an enrichment value, or the normalized $\log_2$ fold change of the number of unique reads mapping to the gene after enrichment relative to the number of reads mapping to that same gene in the input library. The *in vivo* enrichment values for each gene after 2 rounds of enrichment was plotted against the enrichment value for the same gene after 3 rounds of enrichment for wild-type (A) and Δ*caf1* (B) transposon libraries. Genes with enrichment values greater than 2 standard deviations (demarcated with dotted lines) from the mean after both 2 and 3 rounds of enrichment were highlighted. The corresponding *in vitro* enrichment values for each gene highlighted in panels A and B were subtracted from the *in vivo* enrichment values. The 18 genes with positive values are indicated in purple for the wild-type background (C) and 34 genes are indicated in green for the Δ*caf1* background (D). (E) Mutations in six genes were significantly enriched in both the wild-type and Δ*caf1* backgrounds.

adhesins, fimbriae, or other similar structures (33). Instead, these genes are all involved in either the regulation or assembly of macromolecules. The genes *tig*, which encodes trigger factor, and *clpX* both encode proteins that exhibit chaperone functions for structures that assemble in the bacterial cytoplasm (34, 35). The genes *iscR* and *YPO3904* encode transcriptional regulators, *rnc* encodes an endoribonuclease, and *YPO3903* encodes a hypothetical protein. By enriching for mutations in genes that are involved in regulating expression of multiple genes or assembly of multiple proteins, these data suggest that there may be several *Y. pestis* adhesins important for adherence during primary pneumonic plague.

YPO3903 contributes significantly to *Y. pestis* early adherence in the lung. To evaluate the effect on *Y. pestis* adherence for the six significantly enriched mutants in both the wild-type and Δ*caf1* backgrounds, we first created individual clean deletion strains for each gene, except *rnc*, in the wild-type *Y. pestis* background. RNase III, the endoribonuclease encoded by *rnc*, regulates rRNA processing, and *rnc* deletions result in global transcriptome changes that would be difficult to distinguish from other mRNAs that *rnc* may more specifically regulate (36–38). Therefore, due to the global, nonspecific effects of the *rnc* deletion, we chose not to further explore the effects of *rnc* in *Y. pestis* adherence. We inoculated mice intranasally with 1×10^4 CFU of wild-type *Y. pestis* and the Δ*clpX*, Δ*iscR*, and Δ*tig* deletion strains. At 2 hpi, we performed a bronchoalveolar lavage to remove nonadherent bacteria and calculated the proportion of adherent *Y. pestis*. *Y. pestis* Δ*clpX*, *Y. pestis* Δ*iscR*, and *Y. pestis* Δ*tig* all had similar or even slightly higher levels of adherence (65 to 70% adherence) in the lung relative to the ~65% adherence observed for wild-type *Y. pestis* (Fig. 4A). We next inoculated groups of mice with the single-deletion mutants *Y. pestis* Δ*YPO3903* and *Y. pestis* Δ*YPO3904* and compared the adherence at 2 hpi to that in mice inoculated with wild-type *Y. pestis*. *Y. pestis* Δ*YPO3903* had a significant reduction in adherence, with an

TABLE 1 Identity of significantly enriched mutants[a]

| | | | Enrichment value | | | |
| | | | Wild type | | Δcaf1 | |
Locus tag	Gene name	Description	2 rounds	3 rounds	2 rounds	3 rounds
YPO2897	iscR	DNA-binding transcriptional regulator	2.33 (2.32)	2.39 (2.25)	3.01 (2.96)	2.96 (2.93)
YPO3156	clpX	ATP-dependent protease ATP-binding subunit	3.04 (2.93)	3.14 (2.95)	2.75 (2.71)	2.86 (2.61)
YPO3904	hdfR	Transcriptional regulator	3.79 (3.67)	3.96 (3.64)	2.61 (2.15)	2.69 (2.33)
YPO3903		Hypothetical protein	3.65 (3.43)	3.92 (3.47)	3.19 (2.46)	3.39 (2.72)
YPO2718	rnc	Ribonuclease III	3.56 (3.45)	3.75 (3.27)	2.99 (0.06)	3.44 (0.94)
YPO3158	tig	Trigger factor	5.62 (5.06)	5.95 (5.02)	4.15 (3.37)	4.32 (3.59)
YPO3424	nadC	Quinolinate phosphoribosyl-transferase	2.60 (2.29)	2.65 (2.51)	1.51 (1.55)	1.49 (1.60)
YPOs05	micF	sRNA	2.64 (1.40)	2.53 (2.33)	0.00 (0.00)	0.00 (0.00)
YPO3589	pyrI	Aspartate carbamoyltransferase	2.27 (1.94)	2.28 (1.98)	0.83 (−0.12)	1.14 (0.14)
YPO1817		Hypothetical protein	3.53 (2.90)	3.66 (3.34)	−0.33 (−0.57)	−0.06 (−0.12)
YPO0883		DNA binding protein	2.32 (1.79)	2.45 (2.10)	0.09 (0.17)	0.10 (0.23)
YPO3412	speD	S-Adenosylmethionine decarboxylase	2.38 (2.22)	2.55 (2.15)	0.53 (−0.43)	0.76 (0.01)
YPO3880		Hypothetical protein	2.24 (1.48)	2.55 (1.95)	0.34 (0.11)	0.38 (0.25)
YPO2756	mnmC	5-Methylaminomethyl-2-thiouridine methyltransferase	2.46 (1.46)	2.94 (2.00)	0.72 (0.84)	0.66 (0.65)
YPO0416	waaQ	Lipopolysaccharide core biosynthesis protein	7.90 (6.07)	8.05 (6.91)	1.10 (0.00)	1.00 (0.00)
YPt_47		tRNA Arg	2.67 (2.47)	3.43 (2.16)	−1.30 (−1.02)	−0.64 (−1.44)
YPO0650	cca	Multifunctional tRNA nucleotidyl transferase/2′3′-cyclic phosphodiesterase/2′nucleotidase/phosphatase	2.39 (1.53)	2.63 (1.31)	−0.13 (0.24)	−0.27 (0.09)
YPMT1.54		Hypothetical protein	4.06 (3.67)	4.16 (4.13)	0.06 (−1.69)	0.01 (0.21)
YPO3345		Hypothetical protein	−1.18 (−1.38)	−0.99 (−1.20)	4.23 (3.66)	4.09 (4.04)
YPO2503		Hypothetical protein	0.65 (0.41)	0.56 (0.82)	3.35 (3.01)	3.46 (3.31)
YPO1074a		Hypothetical protein	−0.09 (−0.28)	−0.12 (−0.17)	3.34 (2.86)	3.58 (3.33)
YPO1399		Hypothetical protein	−1.25 (−1.05)	−1.02 (−1.36)	4.36 (3.66)	4.59 (4.24)
YPO0135	greB	Transcription elongation factor	6.15 (6.16)	6.25 (6.11)	5.81 (5.26)	5.90 (5.51)
YPO1082	dnaQ	DNA polymerase III subunit epsilon	−1.91 (−1.76)	−1.86 (−1.87)	2.48 (1.25)	2.45 (2.01)
YPO1088		DNA-binding prophage protein	2.53 (2.23)	2.59 (2.67)	3.08 (0.87)	3.31 (2.82)
YPO0393		Hypothetical protein	0.23 (0.25)	0.19 (0.41)	2.92 (2.34)	3.15 (2.64)
YPt_15		Pseudogene	2.27 (2.82)	2.17 (2.50)	2.73 (1.50)	2.99 (2.47)
YPO0019	engB	Ribosome biogenesis GTP-binding protein	0.29 (0.84)	0.20 (0.52)	3.17 (2.68)	3.00 (2.47)
YPO1203a		Hypothetical protein	−0.69 (−0.25)	−0.65 (−0.60)	3.77 (1.25)	3.59 (3.00)
YPO1299	fruK	1-Phosphofructokinase	−1.89 (−1.59)	−2.00 (−1.65)	3.99 (1.68)	4.09 (3.41)
YPO3033		Hypothetical protein	6.29 (6.96)	6.16 (6.57)	6.22 (5.42)	6.56 (5.94)
YPO0901		Hypothetical protein	2.72 (3.32)	2.61 (2.98)	3.07 (2.24)	3.41 (2.74)
YPO2075	rnd	Ribonuclease D	2.61 (2.87)	2.63 (2.67)	3.13 (2.32)	3.26 (2.59)
YPOs02	ssrS	Noncoding RNA	4.12 (4.68)	4.02 (4.35)	3.41 (2.67)	3.56 (2.85)
YPO0060	tdh	L-Threonine 3-dehydrogenase	2.84 (3.46)	2.74 (3.09)	3.59 (2.60)	3.98 (3.23)
YPO2905	ail	Attachment invasion locus	3.96 (4.28)	4.02 (4.35)	3.93 (3.10)	4.34 (3.57)
YPO2235	rnb	Exoribonuclease II	4.57 (4.59)	4.69 (4.54)	4.82 (3.93)	5.14 (4.18)
YPO2621	ubiF	2-Octaprenyl-3-methyl-6-methoxy-1,4-benzoquinol hydroxylase	−1.90 (−1.49)	−1.93 (−1.73)	2.98 (1.25)	3.00 (2.01)
YPO1265		DEAD box helicase family protein	2.97 (3.59)	2.85 (3.23)	4.40 (2.90)	4.88 (3.87)
YPO1681	cheZ	Chemotaxis regulator	2.72 (3.31)	2.69 (2.94)	3.02 (1.51)	3.56 (2.50)
YPO2244	rnfC	Electron transport complex protein	0.24 (0.84)	0.13 (0.49)	3.34 (2.05)	3.70 (2.47)
YPO3587	ptsO	N-regulated PTS system (Npr) phosphohistidinoprotein-hexose phosphotransferase	1.19 (1.00)	1.74 (0.94)	2.75 (0.87)	2.59 (1.33)
YPO2591		Hypothetical protein	1.06 (1.40)	1.17 (1.11)	2.73 (0.00)	3.32 (0.95)
YPO0642		Hypothetical protein	1.70 (2.32)	1.58 (1.96)	4.27 (2.05)	4.52 (1.33)
YPO0480	dapB	Dihydrodipicolinate reductase	−1.08 (−0.74)	−1.18 (−0.84)	2.98 (2.05)	2.81 (2.66)
YPO1704	proQ	Solute/DNA competence effector	3.60 (4.16)	3.52 (3.83)	4.60 (3.90)	4.71 (4.43)

[a]Values are *in vivo* enrichment values for the genes that were >2 SD from the mean and had greater *in vivo* enrichment after two and three rounds of enrichment, with the corresponding *in vitro* values in parentheses. The first group of genes (no highlighting) fit these criteria for both the wild-type and the Δcaf1 backgrounds, the second group (highlighted in light gray) fit these criteria only for the wild-type background, and the third group (highlighted in dark gray) fit these criteria only for the Δcaf1 background.

average of 55% adherence compared to 75% for wild-type *Y. pestis* (Fig. 4B). *Y. pestis* ΔYPO3904 had a small but statistically insignificant reduction in adherence relative to wild-type *Y. pestis* (Fig. 4B). Additionally, each *Y. pestis* strain had a similar total bacterial burden in the lung at 2 hpi, with ~10⁴ CFU recovered (Fig. 4C and D). These data suggest that *YPO3903* plays a significant role in early *Y. pestis* adherence in the lung.
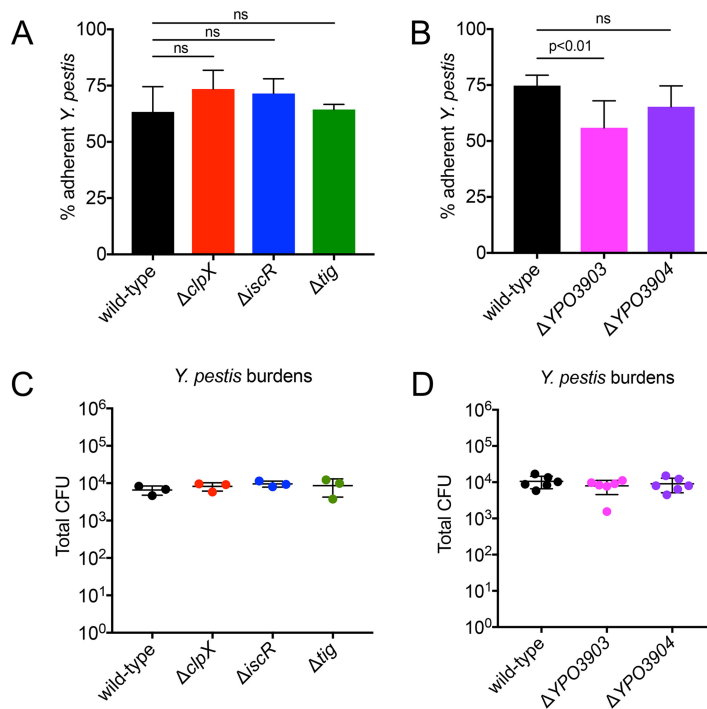
FIG 4 *YPO3903* contributes significantly to *Y. pestis* early adherence in the lung. Mice were inoculated intranasally with 1×10^4 CFU of the *Y. pestis* wild-type, Δ*clpX*, Δ*iscR*, or Δ*tig* strains (A and C) and *Y. pestis* wild-type, Δ*YPO3903*, or Δ*YPO3904* strains (B and D), and bronchoalveolar lavage was performed at 2 hpi. CFU was enumerated in both the BALF and the lung. (A and B) Percent adherence was calculated for each strain by determining the proportion of *Y. pestis* in the lung compared to total CFU in both the BALF and the lung. (C and D) Total *Y. pestis* CFU enumerated in both the lung and the BALF. Data are representative of two independent experiments (A and C) or pooled from two independent experiments (B and D) with 3 mice per group. Data are means and SD. *P* values were determined by one-way ANOVA with Tukey's multiple correction. ns, not significant.

YPO3903 regulates *psaA* levels, which contributes to *Y. pestis* adherence in the lung. Of the five mutations we analyzed for their role in *Y. pestis* adherence *in vivo*, only deletion of *YPO3903* had a significant effect on *Y. pestis* adherence in the lung. We explored the mechanism by which *YPO3903* could modulate adherence in the lung early after inoculation. *YPO3903* encodes a hypothetical protein that has 74% identity to the *Escherichia coli* protein YifE/MaoP (UniProt accession no. A0A384LBX8) (39). MaoP is conserved in *Enterobacteriaceae* and is involved in control of chromosome conformation and segregation (40). As chromosome organization could affect transcription, we hypothesized that the function of YPO3903 could be to regulate the expression of multiple genes involved in *Y. pestis* adherence in the lung. This hypothesis aligns with our prediction that there may be multiple factors involved in mediating adherence in the lung rather than a single *Y. pestis* adhesin.

To test if YPO3903 regulates genes involved in adherence, we measured transcript levels of a small subset of *Y. pestis* genes previously implicated in *in vitro* adherence: *ail*, *caf1*, *pla*, and *psaA* (21, 23, 28). RNA was isolated from wild-type *Y. pestis* or *Y. pestis* Δ*YPO3903* cultures grown at 37°C. The RNA was converted to cDNA, and we performed quantitative reverse transcription-PCR (qRT-PCR) to measure *ail*, *caf1*, *pla*, and *psaA* transcript levels in each strain. While the *ail*, *caf1*, and *pla* transcript levels in Δ*YPO3903* were similar to wild-type levels (no more than a 2-fold change), the levels of *psaA* were reduced over 10-fold in Δ*YPO3903 Y. pestis* relative to the wild-type strain (Fig. 5A). The reduction in *psaA* transcript levels correlated with a loss of PsaA protein levels in Δ*YPO3903 Y. pestis* cultures compared to wild-type *Y. pestis* when strains were grown at 37°C (Fig. S3).

If YPO3903 regulates levels only of *psaA*, we would predict that a *psaA* mutant would be as adherent as a *YPO3903* mutant *in vivo*. If YPO3903 regulates levels of *psaA* in
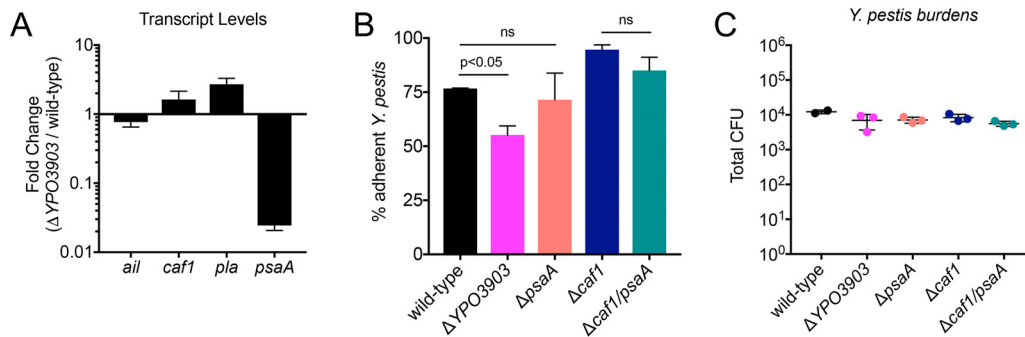
FIG 5 *YPO3903* regulates *psaA* levels, which contributes to *Y. pestis* adherence in the lung. (A) Fold change of transcript levels for *ail*, *caf1*, *pla*, and *psaA* detected by qRT-PCR in Δ*YPO3903* *Y. pestis* relative to the wild-type strain cultured at 37°C. (B and C) Mice were inoculated intranasally with 1×10^4 CFU of the *Y. pestis* wild-type, Δ*YPO3903*, Δ*psaA*, Δ*caf1*, and Δ*caf1* Δ*psaA* strains, and bronchoalveolar lavage was performed at 2 hpi. CFU were enumerated in both the BALF and the lung. (B) Percent adherence was calculated for each strain by determining the proportion of *Y. pestis* in the lung compared to total CFU in both the BALF and the lung. (C) Total *Y. pestis* CFU enumerated in both the lung and the BALF. Data are representative of two independent experiments with 3 mice or replicates per group. Data are means and SD. *P* values were determined by one-way ANOVA with Tukey's multiple correction. ns, not significant.

addition to other genes involved in adherence, we would expect that the loss of *psaA* would have a minor effect on *Y. pestis* adherence *in vivo*. To test the role of *psaA* in *Y. pestis* adherence early during primary pneumonic plague, we inoculated mice intranasally with 1×10^4 CFU wild-type *Y. pestis*, *Y. pestis* Δ*YPO3903*, or *Y. pestis* Δ*psaA*. At 2 hpi, bronchoalveolar lavage was performed, and the proportion of adherent *Y. pestis* bacteria for each strain was calculated. As seen previously, the *YPO3903* mutant had a significant defect in adherence relative to wild-type *Y. pestis*, with approximately 75% adherence calculated for wild-type *Y. pestis* and 55% adherence for Δ*YPO3903* *Y. pestis* (Fig. 5B). However, we observed only a minor loss of adherence in the *psaA* mutant, at ~70% adherence, which was not statistically significant (Fig. 5B). The minor effect of *psaA* on adherence in the lung is also observed in the Δ*caf1* *Y. pestis* background (Fig. 5B). Each strain had a similar total *Y. pestis* burden recovered from the lung at 2 hpi of approximately 10^4 CFU (Fig. 5C). These data support the hypothesis that PsaA contributes to some but not all of the *Y. pestis* adherence in the lung mediated by YPO3903. Thus, YPO3903 controls *Y. pestis* adherence likely by regulating levels of multiple adhesins at the transcriptional level, including *psaA*.

DISCUSSION

Colonization of mucosal surfaces is a critical first step in the pathogenesis of *Yersinia* species. Following inhalation of *Yersinia pestis*, the bacteria colonize the lower airways, where unrestricted bacterial growth during an immunosuppressive phase of disease ultimately leads to severe inflammation and a fatal acute pneumonia (1, 2). Although several proteins have been proposed to mediate adherence *in vitro*, phenotypes for individual mutants are slight and the roles of these proteins in *Y. pestis* adherence in the lung have not been tested. The goal of our study was to identify genes important for *Y. pestis* adherence in the lung during primary pneumonic plague. We used Tn-seq to screen pools of wild-type and Δ*caf1* *Y. pestis* insertional mutants for defects in adherence in the lung.

For our screen, we used a lung lavage assay in which nonadherent bacteria are collected by bronchoalveolar lavage (41). Mutants with insertions in six genes were significantly enriched in both *Y. pestis* strain backgrounds: *YPO3904* and *iscR*, encoding transcriptional regulators; *clpX* and *tig*, encoding proteins that function as molecular chaperones; *rnc*, encoding an endoribonuclease; and *YPO3903*, encoding a hypothetical protein. While none of these genes are annotated to encode adhesins, each one encodes a protein involved in the regulation or assembly of macromolecules. The inactivation of these genes could result in the dysregulation of multiple adhesins. Overall, our Tn-seq results suggest that there may not be one predominant adhesin

that *Y. pestis* utilizes for adherence in the lung. Identification of how each gene regulates the expression, assembly, or display of various surface proteins may reveal the various adhesins *Y. pestis* employs during infection.

A similar serial enrichment strategy was successfully applied to screen *Caulobacter crescentus* transposon mutants for defects in adherence *in vitro*, highlighting the utility of this approach in characterizing bacterial adherence (42). However, in our assay, the enrichment of mutants with transposon insertions in genes involved in gene regulation or protein display rather than adhesins also reflects a limitation of the Tn-seq approach: only single insertional mutants are created by transposon mutagenesis. If there is redundancy among adhesins, or if the loss of a single adhesin can be complemented by the presence of others, then we would not enrich for those particular mutants. Additionally, a unique issue with performing Tn-seq during primary pneumonic plague was identified previously: *Y. pestis* transposon mutants with a wild-type phenotype will transcomplement any avirulent mutants for growth in the lungs (1). The transcomplementation is dependent on the type III secretion system creating a permissive environment in the lungs to allow bacterial outgrowth of avirulent mutants. Since we were evaluating the ability of individual bacterial mutants to bind to the lung epithelium during the first 2 h after inoculation, and because the pCD1⁻ strain was just as adherent as wild-type *Y. pestis*, it is unlikely that transcomplementation affected the results of the screen in this study.

We created clean genetic deletions in our wild-type *Y. pestis* strain for five of the shared enriched mutants to determine their contribution to *Y. pestis* adherence. Of the deletion mutants tested for adherence *in vivo*, only the *YPO3903* mutant had a significant loss of adherence in the lung relative to wild-type *Y. pestis* (Fig. 4). Although *Y. pestis* ΔYPO3904 did not have a statistically significant defect in adherence compared to wild-type *Y. pestis*, it was slightly less adherent in the lung. *YPO3904* encodes a transcriptional regulator with homology to HdfR, which is best characterized for its regulation of the flagellar master operon *flhDC* (43). However, HdfR has flagellum-independent activities, regulating expression of the glutamate synthase gene subunits *gltBD* in *E. coli* and colonization of the bladder during *Proteus mirabilis* infection (44, 45). HdfR may play a minor role in the regulation of genes required for *Y. pestis* adherence. We did not observe any significant loss of adherence for the *clpX*, *iscR*, and *tig* mutants compared to wild-type *Y. pestis*. These genes may play even subtler roles in regulating adherence that could be detectable if the genes were deleted in the more adherent Δcaf1 strain background or when assayed during coinfection with other mutants, similar to the conditions of the Tn-seq screen.

YPO3903 encodes a hypothetical protein, and we determined that YPO3903 has 74% identity to the *E. coli* protein YifE/MaoP. MaoP is conserved in *Enterobacteriaceae* and is involved in control of chromosome conformation and segregation, which can affect gene expression (40, 46). We hypothesized that YPO3903 may perform a similar function in *Y. pestis* and regulate expression or display of adhesins on the cell surface. Transcriptional analyses using quantitative PCR for a small subset of genes previously implicated in *Y. pestis* adherence *in vitro* revealed that transcript levels of *psaA* were about 10-fold lower in the ΔYPO3903 strain than in the wild-type strain (Fig. 5A). The pH 6 antigen, encoded by *psaA*, increases adherence of *Y. pestis* to respiratory epithelial cells by binding phosphatidylcholine, but in the absence of the F1 antigen, a *psaA* mutant is just as adherent as wild-type *Y. pestis* (23, 47). Additionally, a *Y. pestis psaA* mutant has a minor virulence defect in the lung during primary pneumonic plague at 12 hpi that is not sustained as disease progresses (48). We observed a small but statistically insignificant loss of adherence in the lung for a *psaA* mutant in both the wild-type and Δcaf1 *Y. pestis* strains (Fig. 5B). These data again suggest that multiple surface structures may be involved in *Y. pestis* adhesion in the lung and that YPO3903 likely regulates the expression of multiple genes involved in adherence, including *psaA*.

During our *in vivo* screen, we observed strong enrichment of mutants with a Δail colony morphology. This was surprising given our observations that an *ail* mutant was as adherent as wild-type *Y. pestis* early after inoculation (Fig. 1A). However, we observed

a concurrent increase in the prevalence of the Δail colony morphology after in vitro enrichment, particularly in the Δcaf1 background (Fig. 2D). Sequencing results reveal that ail mutants were significantly enriched in the Δcaf1, but not the wild-type, background (Table 1). Therefore, the enrichment of ail mutants in vivo could be due to enhanced growth or enrichment during the in vitro culture steps between passages in mice. Additionally, previous studies using in vitro assays demonstrated moderate defects in Y. pestis adherence to human epithelial cell lines at 37°C when ail was deleted individually, and these defects were enhanced when ail was deleted in combination with other surface protein-encoding genes, such as pla and psaA (16, 21). Taken together, these data suggest that ail may play a minor (if any) role in early Y. pestis adherence in the lung, which was magnified due to enhanced in vitro growth and multiple rounds of enrichment in our screen. The ail gene is one of the most highly expressed genes in Y. pestis at 37°C, and Ail constitutes a large fraction of the outer membrane (19, 49, 50). It is possible that a complete deletion of ail causes disruption of the outer membrane of Y. pestis. Outer membrane perturbations can nonspecifically alter serum sensitivity in E. coli (51). Therefore, the phenotypes we observed for a Y. pestis ail mutant in vitro (loss of adherence and serum sensitivity) may result from outer membrane perturbations due to the loss of Ail. However, molecular analyses of Ail revealed that different residues in the outer loops of the Ail protein contribute to Y. pestis adherence and serum resistance in vitro (52–54). Experiments to determine the role of these adherence-specific residues in vivo would provide a more sophisticated analysis of the contribution of Ail to Y. pestis adherence in the lung without the pleiotropic effects that result from the complete deletion of ail.

Adherence is not completely lost in a Y. pestis YPO3903 mutant, suggesting that there are likely other proteins outside the control of YPO3903 that may play a role in adherence. Although we focused our analysis on the mutations in genes that were enriched in both the wild-type and Δcaf1 backgrounds, there are many mutants with insertions in genes that were significantly enriched and unique to either wild-type or Δcaf1 Y. pestis. We observed a relatively poor correlation between mutants enriched in the wild-type background and those in the caf1 background (Fig. S2). These data imply that the presence of the F1 antigen dramatically alters display or availability of various surface structures for Y. pestis binding to host cells. Because Y. pestis produces the F1 antigen during primary pneumonic plague, mutants that were enriched in the wild-type background may be the most relevant to natural infection. There was significant enrichment of mutations in micF, which is a small regulatory RNA. In Y. pestis, MicF posttranscriptionally regulates levels of OmpF, an outer membrane protein (55). We also observed enrichment of mutations in waaQ, which encodes a lipopolysaccharide core biosynthesis protein (56). Since lipopolysaccharide (LPS) structure can affect the function of outer membrane proteins such as Ail, alterations in LPS resulting from a waaQ mutation may also affect adherence in Y. pestis (30, 57). Mutants with insertions in the gene YPO3880 were also enriched in the wild-type Y. pestis background. YPO3880 is predicted to be an exported protein as part of a chaperone-usher system. The deletion of the operon containing this chaperone-usher system results in slight attenuation of a Y. pestis KIM strain following intranasal, but not intravenous, inoculation (29, 58). Characterizing the genes identified by our in vivo enrichment for nonadherent mutants, as well as further defining the role of YPO3903 in regulating expression of Y. pestis genes involved in adherence, may reveal novel bacterial targets for inhibiting initial Y. pestis colonization of the lung during primary pneumonic plague.

MATERIALS AND METHODS

Bacterial strains and plasmids. The fully virulent Yersinia pestis strain CO92 was obtained from the U.S. Army, Ft. Detrick, MD. The presence of pCD1 and the pgm locus was confirmed by PCR before use. Y. pestis was grown on brain heart infusion (BHI) agar (Difco Laboratories) at 26°C for 2 days. All bacterial strains used in this study are listed in Table S1.

Animals and animal infections. Naive 6- to 8-week-old female C57BL/6J mice were obtained from Jackson Laboratories and housed in animal biosafety level 3 facilities at the University of North Carolina (UNC) at Chapel Hill prior to inoculation. All experiments involving mice were reviewed and approved by the Institutional Animal Care and Use Committee at UNC Chapel Hill under protocol number 15-022 or

number 17-258. *Y. pestis* CO92 growth from a BHI agar plate was used to start liquid cultures in 2 ml BHI broth, which were grown for 12 h at 26°C. Cultures were then diluted 1:200 in 10 ml BHI broth supplemented with 2.5 mM $CaCl_2$ and grown for 12 to 16 h at 37°C with constant shaking at 250 rpm. Mice were lightly anesthetized with 50 to 100 mg/kg ketamine and 5 to 10 mg/kg xylazine and then inoculated intranasally with a lethal dose of bacteria suspended in 20 μl sterile phosphate-buffered saline (PBS). Two hours after inoculation, mice were euthanized with an overdose of sodium pentobarbital.

Determination of nonadherent *Y. pestis*. Groups of mice were euthanized at 2 h postinoculation, and lungs were inflated via tracheal cannulation with 1 ml PBS. The PBS was then retracted to collect bronchoalveolar lavage fluid (BALF). This process was repeated until a total of 3 ml BALF was collected from each mouse. Lungs were then removed, placed in 1 ml PBS, and homogenized with a tissue homogenizer (Dremel). Serial dilutions of both the BALF and lung homogenate were plated on BHI agar to enumerate CFU. To calculate the percent nonadherent *Y. pestis*, the number of CFU in the BALF was divided by the sum of CFU in the lung homogenate and the BALF.

Transposon mutagenesis. The transposon mutant libraries were generated using the *Himar1*-based transposon system encoded on pPP47, which has been used previously for transposon mutagenesis in *Yersinia pestis* (1). *E. coli* S17 λpir carrying pPP47 was mated with *Y. pestis* wild-type and Δcaf1 strains twice. A 500-μl portion of liquid culture for each strain was washed with 1 ml 10 mM $MgSO_4$, and then each *Y. pestis* strain was combined with *E. coli* in 50 μl 10 mM $MgSO_4$, and this mixture was spotted on BHI agar. The wild-type *Y. pestis* transposon libraries are designated YP473Tn and the Δcaf1 *Y. pestis* transposon libraries are designated YP475Tn. For YP473Tn and YP475Tn libraries, only one mating was performed for each strain. For YP473Tn3 and YP475Tn2 libraries, 4 individual matings were performed for each strain. Plates were incubated for 5 h at 26°C. A cotton swab was used to collect the resulting bacterial growth from each plate, which was resuspended in 1 ml PBS. For YP473Tn and YP475Tn, this was diluted 1:100 in PBS, and 250 μl was plated on 5 BHI agar plates containing kanamycin for *Y. pestis* selection with the transposon integrated into the genome and polymyxin B for *E. coli* counterselection. For YP473Tn3 and YP475Tn2, the resuspended mating was diluted 1:10 in PBS, and 200 μl was plated on 8 BHI agar plates with kanamycin and polymyxin B. Serial dilutions were also plated for each mating resuspension to determine the concentration of mutants in each mating. After 2 days incubation at 26°C, colonies were collected from the plates by flooding the top of the plate with BHI broth and dislodging colonies with a cell spreader. The medium was removed with a serological pipet and pooled in a 50-ml conical tube. Approximately 48,000 individual colonies for YP473Tn, ~43,000 colonies for YP475Tn, ~185,920 colonies for YP473Tn3, and ~165,760 colonies for YP475Tn2 were collected. The colonies were resuspended in the BHI broth by repeated pipetting, and glycerol was added to a final concentration of 15%. Aliquots (500 μl) of each mating were kept at −80°C until use.

Enrichment of transposon mutants *in vivo* and *in vitro*. For the following protocol, the BHI agar or liquid broth used was supplemented with kanamycin (50 μg/ml) to maintain selection of transposon insertional mutants (kanamycin resistance). One frozen library aliquot from each transposon mutagenesis library (YP473Tn and YP473Tn3 for the wild-type background and YP475Tn and YP475Tn3 for the Δcaf1 background) was thawed. YP473Tn was mixed with YP473Tn3 and YP475Tn was mixed with YP475Tn2. A 500-μl portion of the combined transposon libraries was added to separate 10-ml BHI broth cultures supplemented with 1 mM $CaCl_2$ to generate the wild-type (WT) input (YP473Tn+YP473Tn3) and the Caf1 input (YP475Tn+YP475Tn2). The two libraries from the separate matings were combined to maximize diversity of insertional mutants in both input libraries. These cultures were incubated shaking at 37°C for 4 h. A 200-μl portion of each culture was added to 10 ml of fresh BHI broth supplemented with 1 mM $CaCl_2$ and incubated with shaking for 15 h. The optical density at 620 nm (OD_{620}) for each culture was determined, and 2 groups (designated WT *in vivo* group 1 and group 2) of 3 mice each were inoculated intranasally with 1×10^6 CFU WT input, and 2 groups (designated Caf1 *in vivo* group 1 and group 2) of 3 mice each were inoculated intranasally with 5×10^6 CFU Caf1 input. At the same time, 200 μl of the WT and Caf1 input cultures were added to 2 separate flasks of 10 ml BHI broth supplemented with 1 mM $CaCl_2$ and were incubated with shaking at 37°C. Each flask was designated WT or Caf1 *in vitro* group 1 or group 2. At 2 hpi, mice were euthanized, lungs were inflated via tracheal cannulation with 1 ml ice-cold PBS, and the liquid was retracted to collect BALF. A total of 3 ml BALF was collected from each mouse. Lungs were then removed, placed in 1 ml PBS, and homogenized with a tissue homogenizer (Dremel). Serial dilutions of both the BALF and lung homogenate were made and plated on BHI agar to enumerate CFU. The remaining BALF (containing nonadherent *Y. pestis* mutants) was plated on BHI agar. The OD_{620} was determined for the *in vitro* cultures and 1×10^6 CFU from each was diluted in 1 ml PBS and plated on BHI agar.

After 2 days of incubation at 26°C, the single colonies were collected from each plate. For each set of plates from a single mouse, BHI broth was poured on the surface of the agar plates. A plate spreader was used to dislodge the colonies from the surface of the agar into the medium, and this was collected with a serological pipet. The colony suspension was transferred to a 50-ml conical tube. This process was repeated for each set of plates from each mouse and each *in vitro* group. The colony suspensions for the 3 mice from group 1 were pooled, and the suspensions from group 2 were pooled for both the WT and Caf1 libraries. The colony suspensions from *in vitro* groups 1 and 2 were kept separate. A 500-μl portion of each pooled suspension was added to 500 μl of 50% glycerol and kept at −80°C. The strains generated from freezing aliquots of each library after enrichment are listed in Table S2. A 500-μl portion of each pooled bacterial suspension was added to 10 ml of fresh BHI broth with $CaCl_2$ and incubated with shaking at 37°C for 4 h. Then, 200 μl of each culture was added to 10 ml of fresh BHI broth with $CaCl_2$ and shaking at 37°C for 15 h. The process of inoculating groups of mice and the *in vitro* cultures and collecting mutants was repeated for a total of 4 rounds of enrichment *in vivo* and *in vitro*.

Preparation of bacterial genomes for sequencing. Frozen aliquots of the WT and Caf1 libraries before, during, and after enrichment were thawed, and 500 μl of the stock was added to 10 ml BHI broth and grown with shaking at 37°C for 6 h. A 500-μl portion of this culture was added to fresh 10 ml BHI broth and grown shaking at 37°C for 12 h. Genomic DNA was isolated from 500 μl of culture using the Wizard Genomic DNA purification kit (Promega) following the manufacturer's protocols. The names of all samples of DNA isolated from the corresponding pool of transposon mutants are listed in Table S2. Each DNA pellet was rehydrated overnight in 100 μl Tris-EDTA (TE) buffer at 4°C. An additional 100 μl TE buffer was added to each genomic DNA sample; then each sample was sheared using an EpiShear Probe sonicator (Active Motif) with 1 s on/1 s off for 30 s at 30% amplitude for 6 cycles, with 1 min of incubation on ice between cycles. Following sonication, each sample was purified using PCR purification with a QiaQuick kit (Qiagen) and eluted in 50 μl nuclease-free distilled H$_2$O (dH$_2$O). Samples were stored at −20°C until preparation for sequencing.

Each sheared DNA sample was diluted to 250 ng in a total volume of 50 μl nuclease-free dH$_2$O. The KAPA Hyper Prep kit (KAPA Biosystems) was used to perform end repair, A-tailing, and adaptor ligation for each sample. Seven microliters of end repair and A-tailing buffer and 3 μl of end repair and A-tailing enzyme mix were added to the sheared DNA samples. The following thermocycler program was run: 30 min at 20°C, 30 min at 65°C, then hold at 4°C. Next, adaptor ligation was performed. The end repair and A-tailing product was added to 30 μl ligation buffer, 10 μl DNA ligase, 5 μl PCR water, and 5 μl of a 15 μM mix of adaptors A01 and A02. These samples were incubated at 20°C for 15 min. A postligation bead cleanup was performed using Agencourt AMPure XP beads, using a 0.8× bead selection according to the manufacturer's protocols. The sample was eluted in 50 μl buffer EB (10 mM Tris-Cl, pH 8.5). A second bead cleanup was immediately performed with a 1× bead selection and elution of the DNA in 20 μl buffer EB. The samples were kept at −20°C until the PCRs.

PCR to amplify the transposon junctions was performed using the KAPA Robust 2G kit (KAPA Biosystems). The first PCR amplified sheared DNA sequences that had successfully ligated the adaptors. The 20-μl sample created with the KAPA Hyper Prep kit was added to 10 μl 5× buffer A, 5× enhancer, 10 mM deoxynucleoside triphosphates (dNTPs), 5 μM primer R1, 5 μM primer KAPA Prim 1, and 0.2 μl polymerase. The reaction was run in a thermocycler with the following program: 1 cycle of 98°C for 45 s; 10 cycles of 98°C for 15 s, 55°C for 30 s, and 72°C for 30 s; 1 cycle of 72°C for 1 min; then a hold at 4°C. A bead cleanup was performed for each sample with Agencourt beads, using a 1× bead selection according to the manufacturer's protocols and eluting in 20 μl buffer EB. The second PCR further amplified the read fragments and added the sample-specific barcode sequence to allow pooling of the libraries for sequencing. This PCR was performed using KAPA HiFi *Taq* from the KAPA Hyper Prep kit (KAPA Biosystems). The 20-μl sample from the previous bead cleanup was added to 25 μl Ready Mix (2×), 5 μM index primer, and 5 μM primer KAPA Prim 1. The index primer used for each library is listed in Table S2. The reaction was run in a thermocycler with the following protocol: 1 cycle of 98°C for 45 s; 3 cycles of 98°C for 15 s, 63°C for 30 s, and 72°C for 15 s; 10 cycles of 98°C for 15 s, 65°C for 30 s, and 72°C for 30 s; 1 cycle of 72°C for 1 min; then a hold at 4°C. A bead cleanup was performed for each sample with Agencourt beads, using a 1× bead selection according to the manufacturer's protocols and eluting in 20 μl buffer EB.

Each sample was analyzed on a Bioanalyzer (Agilent) to determine the molarity of the amplicons in the size range of 350 to 600 bp, which was the desired range of fragment lengths for sequencing. Each sample was diluted to 15 nM, and 5-μl portions of each sample was pooled, yielding a pooled sample volume of 90 μl. A double size selection was performed on the pooled sample using a 0.5 to 0.7× bead ratio with Agencourt beads following the manufacturer's protocol. The double size selection further enriched the pooled sample for amplicons ranging from 200 to 800 bp. The sample was eluted in buffer EB, the concentration was determined by Qubit analysis, and the molarity was determined with a Bioanalyzer (Agilent). The sample was diluted to a final concentration of 30 nM in a 25-μl volume of buffer EB, which was sequenced using the Illumina MiSeq with 150× paired-end reads.

Analysis of transposon mutants. (i) Read count and normalization. The paired end reads generated 2 FASTQ files for each amplicon sequenced, named Read 1 (R1) and Read 2 (R2). Each read in the R2 FASTQ file was modified such that the four random nucleotides (NNNN in primer R1, which creates a random barcode to aid in identification of PCR duplicates), were removed and appended to the R2 identifier line. BWA (Burrows-Wheeler alignment tool) alignment (v0.7.17-r1194-dirty) to the *Yersinia pestis* CO92 full genome (33) was then performed on each paired-end set of FASTQ files and sorted using samtools (v1.8), after which duplicates were filtered using biobambam's bammarkduplicate program (v2.0.33). This generated SAM (sequence alignment/map) files for each read.

Reads from the duplicate-filtered alignment were then inspected to find the insertion locations of the transposon. Most alignments allowed quick determination of the transposon insertion site, where a TA/AT dinucleotide was present followed by the transposon sequence. Other alignments resulted in a portion of the end sequence of the transposon aligning to the genome, thus obscuring the true start site. These states were suggested by the presence of soft clips adjacent to a match (denoted by an *n*S*n*M, *n*M*n*S, or *n*S*n*M*n*S pattern in the CIGAR string, where *n* denotes the number of nucleotides to which the designation of S, denoting a soft clip, or M, denoting a match, applies) of reads in the SAM file.

To confirm each suggested location, NCBI's BLASTn (ncbi-blast v2.7.1+) program was used to determine the true start site of transposon insertion, where BLASTn was run with the transposon sequence against each of the suggested reads. BLAST, being a greedy aligner, would give results matching the entire transposon sequence if possible. For reads for which there was only an *n*M pattern in the CIGAR string, BLASTn would return a position such that the transposon insertion position complemented the start of the read as reported by BWA. For instances where a read's CIGAR string

contained a combination of soft clips and matches, any unaligned portion from BLASTn could be truly attributable to the *Y. pestis* genome. This allowed the resolution between BWA's reported read and the exact location of the transposon insertion site in the genome. The number of unique insertions for each gene was quantified, and upper-quartile normalization was performed to give a read count for each gene.

(ii) Calculating top hits. The normalized read counts for each gene were averaged between the replicate samples, and this average was divided by the normalized read count for the input library and $\log_2$ transformed to give an output/input ratio for the following groups: WT *in vivo* 2 rounds, WT *in vivo* 3 rounds, WT *in vitro* 2 rounds, WT *in vitro* 3 rounds, Caf1 *in vivo* 2 rounds, Caf1 *in vivo* 3 rounds, Caf1 *in vitro* 2 rounds, and Caf1 *in vitro* 3 rounds. The mean and standard deviation of the output/input ratios for every gene within each individual group were calculated. Genes that were more than 2 standard deviations away from the mean in both *in vivo* 2 rounds or *in vivo* 3 were pursued for further analysis.

Lambda red recombination. Deletion of *clpX*, *iscR*, *tig*, *YPO3903*, and *YPO3904* was performed in *Y. pestis* wild-type and pCD1− backgrounds using a modified form of lambda red recombination. Briefly, 500 bp upstream and 500 bp downstream sequences for the desired region to delete were amplified by PCR and combined in splicing by overhang extension (SOE) PCR with a Kan^r cassette flanked by FLP recombination target (FRT) sites for allelic replacement of the wild-type open reading frame (ORF) (59). The products were transformed into *Y. pestis* strains harboring pWL204, a plasmid containing the recombinase genes (10). Following successful recombination verified by PCR, the Kan^r cassette was resolved by the introduction of pSkippy, a Tet^s derivative of pFLP3 harboring an Amp^r cassette and *sacB* and carrying the FLP recombinase gene under the control of the *lac* promoter (60). Correct resolution of the Kan^r cassette, as well as presence of the virulence plasmids (for mutants in the *Y. pestis* wild-type background) and the *pgm* locus, was confirmed by PCR. The oligonucleotides used for lambda red recombination and the strains generated are listed in Table S1.

Transcript quantification by qRT-PCR. Two-milliliter portions of BHI broth cultures were inoculated with either wild-type or Δ*YPO3903 Y. pestis* in the pCD1− background and incubated with rolling overnight at 26°C. A 250-μl portion of each culture was added to 10 ml of fresh BHI broth supplemented with 1 mM CaCl$_2$ and incubated with shaking for 6 h at 37°C. Total RNA was then purified from 1 ml of culture using the TRIzol reagent manufacturer's protocol, treated with Turbo DNase (Ambion), and reverse transcribed with the iScript cDNA synthesis kit (Bio-Rad) according to the manufacturer's instructions. cDNAs were used as the templates for amplification and detection of the *Y. pestis* genes *ail*, *caf1*, *pla*, and *psaA* with SYBR green dye (Bio-Rad) in an iCycler thermocycler (Bio-Rad). For each gene, the calculated threshold cycle (C_T) was normalized to that of gyrase B (*gyrB*) from the same sample prior to calculation of the fold change using the $\Delta\Delta C_T$ method (61). Oligonucleotides used for qRT-PCR are listed in Table S1.

Western blot analysis. Two-milliliter portions of BHI broth cultures were inoculated with either wild-type or Δ*YPO3903 Y. pestis* in the pCD1− background and incubated with rolling overnight at 26°C. A 250-μl portion of each culture was added to 10 ml of fresh BHI broth supplemented with 1 mM CaCl$_2$ and incubated with shaking for 6 h at 26°C or 37°C. Whole-cell lysates were prepared from cells at an OD$_{620}$ of 2 that had been pelleted, washed once with ice-cold PBS, and resuspended in Laemmli buffer containing 5% β-mercaptoethanol. Samples were boiled for 10 min, and a portion corresponding to an OD$_{620}$ of 0.2 was separated via SDS-PAGE and transferred to polyvinylidene difluoride (PVDF) membranes for Western blot analysis. Loading was qualitatively assessed by Ponceau S staining of the PVDF membrane. Anti-PsaA serum was used to probe for PsaA. Prior to use, the anti-PsaA serum was absorbed against *E. coli* lysates and used at a titer of 1:2,500 (62). Anti-IgG horseradish peroxidase (HRP)-conjugated secondary antibodies were used at a titer of 1:20,000.

Statistical analysis. Data were graphed and analyzed for statistical significance in Prism 7.0b. Data were analyzed by one-way analysis of variance (ANOVA) with Tukey's multiple-comparison test or by Student's *t* test and are presented as means with standard deviations (SD). Details for statistical analyses, such as numbers of replicates, group numbers, the statistical test used, and the definition of statistical significance, are given in the figure legends.

SUPPLEMENTAL MATERIAL

Supplemental material is available online only.

FIG S1, PDF file, 2.4 MB.

FIG S2, PDF file, 0.7 MB.

FIG S3, PDF file, 0.6 MB.

TABLE S1, DOCX file, 0.03 MB.

TABLE S2, DOCX file, 0.01 MB.

ACKNOWLEDGMENTS

The content is solely the responsibility of the authors and does not necessarily represent the official views of the National Institutes of Health.

REFERENCES

1. Price PA, Jin J, Goldman WE. 2012. Pulmonary infection by *Yersinia pestis* rapidly establishes a permissive environment for microbial proliferation. Proc Natl Acad Sci U S A 109:3083–3088. https://doi.org/10.1073/pnas.1112729109.

2. Lathem WW, Crosby SD, Miller VL, Goldman WE. 2005. Progression of primary pneumonic plague: a mouse model of infection, pathology, and bacterial transcriptional activity. Proc Natl Acad Sci U S A 102:17786–17791. https://doi.org/10.1073/pnas.0506840102.

3. Beachey EH. 1981. Bacterial adherence: adhesin-receptor interactions mediating the attachment of bacteria to mucosal surface. J Infect Dis 143:325–345. https://doi.org/10.1093/infdis/143.3.325.

4. Davis KM. 2018. All *Yersinia* are not created equal: phenotypic adaptation to distinct niches within mammalian tissues. Front Cell Infect Microbiol 8:261. https://doi.org/10.3389/fcimb.2018.00261.

5. Isberg RR, Barnes P. 2001. Subversion of integrins by enteropathogenic *Yersinia*. J Cell Sci 114:21–28.

6. Heise T, Dersch P. 2006. Identification of a domain in *Yersinia* virulence factor YadA that is crucial for extracellular matrix-specific cell adhesion and uptake. Proc Natl Acad Sci U S A 103:3375–3380. https://doi.org/10.1073/pnas.0507749103.

7. Mikula KM, Kolodziejczyk R, Goldman A. 2012. *Yersinia* infection tools—characterization of structure and function of adhesins. Front Cell Infect Microbiol 2:169. https://doi.org/10.3389/fcimb.2012.00169.

8. Rosqvist R, Skurnik M, Wolf-Watz H. 1988. Increased virulence of *Yersinia pseudotuberculosis* by two independent mutations. Nature 334:522–524. https://doi.org/10.1038/334522a0.

9. Isberg RR, Falkow S. 1985. A single genetic locus encoded by *Yersinia pseudotuberculosis* permits invasion of cultured animal cells by *Escherichia coli* K-12. Nature 317:262–264. https://doi.org/10.1038/317262a0.

10. Lathem WW, Price PA, Miller VL, Goldman WE. 2007. A plasminogen-activating protease specifically controls the development of primary pneumonic plague. Science 315:509–513. https://doi.org/10.1126/science.1137195.

11. Caulfield AJ, Lathem WW. 2012. Substrates of the plasminogen activator protease of *Yersinia pestis*. Adv Exp Med Biol 954:253–260. https://doi.org/10.1007/978-1-4614-3561-7_32.

12. Lähteenmäki K, Virkola R, Sarén A, Emödy L, Korhonen TK. 1998. Expression of plasminogen activator Pla of *Yersinia pestis* enhances bacterial attachment to the mammalian extracellular matrix. Infect Immun 66:5755–5762. https://doi.org/10.1128/IAI.66.12.5755-5762.1998.

13. Cowan C, Jones HA, Kaya YH, Perry RD, Straley SC. 2000. Invasion of epithelial cells by *Yersinia pestis*: evidence for a *Y. pestis*-specific invasin. Infect Immun 68:4523–4530. https://doi.org/10.1128/iai.68.8.4523-4530.2000.

14. Banerjee SK, Huckuntod SD, Mills SD, Kurten RC, Pechous RD. 2019. Modeling pneumonic plague in human precision-cut lung slices highlights a role for the plasminogen activator protease in facilitating type 3 secretion. Infect Immun 87:e00175-19. https://doi.org/10.1128/IAI.00175-19.

15. Banerjee SK, Crane SD, Pechous RD. 2020. A dual role for the plasminogen activator protease during the pre-inflammatory phase of primary pneumonic plague. J Infect Dis 222:407–416. https://doi.org/10.1093/infdis/jiaa094.

16. Felek S, Tsang TM, Krukonis ES. 2010. Three *Yersinia pestis* adhesins facilitate Yop delivery to eukaryotic cells and contribute to plague virulence. Infect Immun 78:4134–4150. https://doi.org/10.1128/IAI.00167-10.

17. Bliska JB, Falkow S. 1992. Bacterial resistance to complement killing mediated by the Ail protein of *Yersinia enterocolitica*. Proc Natl Acad Sci U S A 89:3561–3565. https://doi.org/10.1073/pnas.89.8.3561.

18. Yang Y, Merriam JJ, Mueller JP, Isberg RR. 1996. The *psa* locus is responsible for thermoinducible binding of *Yersinia pseudotuberculosis* to cultured cells. Infect Immun 64:2483–2489. https://doi.org/10.1128/IAI.64.7.2483-2489.1996.

19. Bartra SS, Styer KL, O'Bryant DM, Nilles ML, Hinnebusch BJ, Aballay A, Plano GV. 2008. Resistance of *Yersinia pestis* to complement-dependent killing is mediated by the Ail outer membrane protein. Infect Immun 76:612–622. https://doi.org/10.1128/IAI.01125-07.

20. Pierson DE, Falkow S. 1993. The *ail* gene of *Yersinia enterocolitica* has a role in the ability of the organism to survive serum killing. Infect Immun 61:1846–1852. https://doi.org/10.1128/IAI.61.5.1846-1852.1993.

21. Felek S, Krukonis ES. 2009. The *Yersinia pestis* Ail protein mediates binding and Yop delivery to host cells required for plague virulence. Infect Immun 77:825–836. https://doi.org/10.1128/IAI.00913-08.

22. Lindler LE, Klempner MS, Straley SC. 1990. *Yersinia pestis* pH 6 antigen: genetic, biochemical, and virulence characterization of a protein involved in the pathogenesis of bubonic plague. Infect Immun 58:2569–2577. https://doi.org/10.1128/IAI.58.8.2569-2577.1990.

23. Liu F, Chen H, Galván EM, Lasaro MA, Schifferli DM. 2006. Effects of Psa and F1 on the adhesive and invasive interactions of *Yersinia pestis* with human respiratory tract epithelial cells. Infect Immun 74:5636–5644. https://doi.org/10.1128/IAI.00612-06.

24. Huang X-Z, Lindler LE. 2004. The pH 6 antigen is an antiphagocytic factor produced by *Yersinia pestis* independent of *Yersinia* outer proteins and capsule antigen. Infect Immun 72:7212–7219. https://doi.org/10.1128/IAI.72.12.7212-7219.2004.

25. Perry RD, Fetherston JD. 1997. *Yersinia pestis*—etiologic agent of plague. Clin Microbiol Rev 10:35–66. https://doi.org/10.1128/CMR.10.1.35.

26. Galyov EE, Smirnov OYu, Karlishev AV, Volkovoy KI, Denesyuk AI, Nazimov IV, Rubtsov KS, Abramov VM, Dalvadyanz SM, Zav'yalov VP. 1990. Nucleotide sequence of the *Yersinia pestis* gene encoding F1 antigen and the primary structure of the protein. Putative T and B cell epitopes. FEBS Lett 277:230–232. https://doi.org/10.1016/0014-5793(90)80852-A.

27. Du Y, Rosqvist R, Forsberg A. 2002. Role of fraction 1 antigen of *Yersinia pestis* in inhibition of phagocytosis. Infect Immun 70:1453–1460. https://doi.org/10.1128/iai.70.3.1453-1460.2002.

28. Runco LM, Myrczek S, Bliska JB, Thanassi DG. 2008. Biogenesis of the fraction 1 capsule and analysis of the ultrastructure of *Yersinia pestis*. J Bacteriol 190:3381–3385. https://doi.org/10.1128/JB.01840-07.

29. Hatkoff M, Runco LM, Pujol C, Jayatilaka I, Furie MB, Bliska JB, Thanassi DG. 2012. Roles of chaperone/usher pathways of *Yersinia pestis* in a murine model of plague and adhesion to host cells. Infect Immun 80:3490–3500. https://doi.org/10.1128/IAI.00434-12.

30. Kolodziejek AM, Schnider DR, Rohde HN, Wojtowicz AJ, Bohach GA, Minnich SA, Hovde CJ. 2010. Outer membrane protein X (Ail) contributes to *Yersinia pestis* virulence in pneumonic plague and its activity is dependent on the lipopolysaccharide core length. Infect Immun 78:5233–5243. https://doi.org/10.1128/IAI.00783-10.

31. Osei-Owusu P, Charlton TM, Kim HK, Missiakas D, Schneewind O. 2019. FPR1 is the plague receptor on host immune cells. Nature 574:57–24. https://doi.org/10.1038/s41586-019-1570-z.

32. Palace SG, Proulx MK, Lu S, Baker RE, Goguen JD. 2014. Genome-wide mutant fitness profiling identifies nutritional requirements for optimal growth of *Yersinia pestis* in deep tissue. mBio 5:e01385-14. https://doi.org/10.1128/mBio.01385-14.

33. Parkhill J, Wren BW, Thomson NR, Titball RW, Holden MT, Prentice MB, Sebaihia M, James KD, Churcher C, Mungall KL, Baker S, Basham D, Bentley SD, Brooks K, Cerdeño-Tárraga AM, Chillingworth T, Cronin A, Davies RM, Davis P, Dougan G, Feltwell T, Hamlin N, Holroyd S, Jagels K, Karlyshev AV, Leather S, Moule S, Oyston PC, Quail M, Rutherford K, Simmonds M, Skelton J, Stevens K, Whitehead S, Barrell BG. 2001. Genome sequence of *Yersinia pestis*, the causative agent of plague. Nature 413:523–527. https://doi.org/10.1038/35097083.

34. Wawrzynow A, Wojtkowiak D, Marszalek J, Banecki B, Jonsen M, Graves B, Georgopoulos C, Zylicz M. 1995. The ClpX heat-shock protein of *Escherichia coli*, the ATP-dependent substrate specificity component of the ClpP-ClpX protease, is a novel molecular chaperone. EMBO J 14:1867–1877. https://doi.org/10.1002/j.1460-2075.1995.tb07179.x.

35. Hoffmann A, Bukau B, Kramer G. 2010. Structure and function of the molecular chaperone trigger factor. Biochim Biophys Acta 1803:650–661. https://doi.org/10.1016/j.bbamcr.2010.01.017.

36. Lawal A, Jejelowo O, Chopra AK, Rosenzweig JA. 2011. Ribonucleases and bacterial virulence. Microb Biotechnol 4:558–571. https://doi.org/10.1111/j.1751-7915.2010.00212.x.

37. Court DL, Gan J, Liang Y-H, Shaw GX, Tropea JE, Costantino N, Waugh DS, Ji X. 2013. RNase III: genetics and function; structure and mechanism. Annu Rev Genet 47:405–431. https://doi.org/10.1146/annurev-genet-110711-155618.

38. Sim S-H, Yeom J-H, Shin C, Song W-S, Shin E, Kim H-M, Cha C-J, Han SH, Ha N-C, Kim SW, Hahn Y, Bae J, Lee K. 2010. *Escherichia coli* ribonuclease III activity is downregulated by osmotic stress: consequences for the degradation of *bdm* mRNA in biofilm formation. Mol Microbiol 75:413–425. https://doi.org/10.1111/j.1365-2958.2009.06986.x.

39. UniProt Consortium. 2019. UniProt: a worldwide hub of protein knowledge. Nucleic Acids Res 47:D506–D515. https://doi.org/10.1093/nar/gky1049.

40. Valens M, Thiel A, Boccard F. 2016. The MaoP/*maoS* site-specific system organizes the Ori region of the *E. coli* chromosome into a macrodomain. PLoS Genet 12:e1006309. https://doi.org/10.1371/journal.pgen.1006309.

41. Scheller EV, Melvin JA, Sheets AJ, Cotter PA. 2015. Cooperative roles for fimbria and filamentous hemagglutinin in *Bordetella* adherence and immune modulation. mBio 6:e00500-15. https://doi.org/10.1128/mBio.00500-15.

42. Hershey DM, Fiebig A, Crosson S. 2019. A genome-wide analysis of adhesion in *Caulobacter crescentus* identifies new regulatory and biosynthetic components for holdfast assembly. mBio 10:e02273-18. https://doi.org/10.1128/mBio.02273-18.

43. Ko M, Park C. 2000. H-NS-dependent regulation of flagellar synthesis is mediated by a LysR family protein. J Bacteriol 182:4670–4672. https://doi.org/10.1128/jb.182.16.4670-4672.2000.

44. Krin E, Danchin A, Soutourina O. 2010. Decrypting the H-NS-dependent regulatory cascade of acid stress resistance in *Escherichia coli*. BMC Microbiol 10:273. https://doi.org/10.1186/1471-2180-10-273.

45. Burall LS, Harro JM, Li X, Lockatell CV, Himpsl SD, Hebel JR, Johnson DE, Mobley HLT. 2004. *Proteus mirabilis* genes that contribute to pathogenesis of urinary tract infection: identification of 25 signature-tagged mutants attenuated at least 100-fold. Infect Immun 72:2922–2938. https://doi.org/10.1128/iai.72.5.2922-2938.2004.

46. Dame RT, Rashid F-ZM, Grainger DC. 2020. Chromosome organization in bacteria: mechanistic insights into genome structure and function. Nat Rev Genet 21:227–242. https://doi.org/10.1038/s41576-019-0185-4.

47. Galván EM, Chen H, Schifferli DM. 2007. The Psa fimbriae of *Yersinia pestis* interact with phosphatidylcholine on alveolar epithelial cells and pulmonary surfactant. Infect Immun 75:1272–1279. https://doi.org/10.1128/IAI.01153-06.

48. Weening EH, Cathelyn JS, Kaufman G, Lawrenz MB, Price P, Goldman WE, Miller VL. 2011. The dependence of the *Yersinia pestis* capsule on pathogenesis is influenced by the mouse background. Infect Immun 79:644–652. https://doi.org/10.1128/IAI.00981-10.

49. Kolodziejek AM, Hovde CJ, Minnich SA. 2012. *Yersinia pestis* Ail: multiple roles of a single protein. Front Cell Infect Microbiol 2:103. https://doi.org/10.3389/fcimb.2012.00103.

50. Myers-Morales T, Cowan C, Gray ME, Wulff CR, Parker CE, Borchers CH, Straley SC. 2007. A surface-focused biotinylation procedure identifies the *Yersinia pestis* catalase KatY as a membrane-associated but non-surface-located protein. Appl Environ Microbiol 73:5750–5759. https://doi.org/10.1128/AEM.02968-06.

51. Miajlovic H, Smith SG. 2014. Bacterial self-defence: how *Escherichia coli* evades serum killing. FEMS Microbiol Lett 354:1–9. https://doi.org/10.1111/1574-6968.12419.

52. Miller VL, Beer KB, Heusipp G, Young BM, Wachtel MR. 2001. Identification of regions of Ail required for the invasion and serum resistance phenotypes. Mol Microbiol 41:1053–1062. https://doi.org/10.1046/j.1365-2958.2001.02575.x.

53. Tsang TM, Wiese JS, Alhabeil JA, Usselman LD, Thomson JJ, Matti R, Kronshage M, Maricic N, Williams S, Sleiman NH, Felek S, Krukonis ES. 2017. Defining the Ail ligand-binding surface: hydrophobic residues in two extracellular loops mediate cell and extracellular matrix binding to facilitate Yop delivery. Infect Immun 85:e01047-15. https://doi.org/10.1128/IAI.01047-15.

54. Thomson JJ, Plecha SC, Krukonis ES. 2019. Ail provides multiple mechanisms of serum resistance to *Yersinia pestis*. Mol Microbiol 111:82–95. https://doi.org/10.1111/mmi.14140.

55. Liu Z, Wang H, Wang H, Wang J, Bi Y, Wang X, Yang R, Han Y. 2015. Intrinsic plasmids influence MicF-mediated translational repression of *ompF* in *Yersinia pestis*. Front Microbiol 6:862. https://doi.org/10.3389/fmicb.2015.00862.

56. Kiljunen S, Datta N, Dentovskaya SV, Anisimov AP, Knirel YA, Bengoechea JA, Holst O, Skurnik M. 2011. Identification of the lipopolysaccharide core of *Yersinia pestis* and *Yersinia pseudotuberculosis* as the receptor for bacteriophage φA1122. J Bacteriol 193:4963–4972. https://doi.org/10.1128/JB.00339-11.

57. Pierson DE. 1994. Mutations affecting lipopolysaccharide enhance Ail-mediated entry of *Yersinia enterocolitica* into mammalian cells. J Bacteriol 176:4043–4051. https://doi.org/10.1128/jb.176.13.4043-4051.1994.

58. Felek S, Jeong JJ, Runco LM, Murray S, Thanassi DG, Krukonis ES. 2011. Contributions of chaperone/usher systems to cell binding, biofilm formation and *Yersinia pestis* virulence. Microbiology 157:805–818. https://doi.org/10.1099/mic.0.044826-0.

59. Datsenko KA, Wanner BL. 2000. One-step inactivation of chromosomal genes in *Escherichia coli* K-12 using PCR products. Proc Natl Acad Sci U S A 97:6640–6645. https://doi.org/10.1073/pnas.120163297.

60. Choi K-H, Gaynor JB, White KG, Lopez C, Bosio CM, Karkhoff-Schweizer RR, Schweizer HP. 2005. A Tn7-based broad-range bacterial cloning and expression system. Nat Methods 2:443–448. https://doi.org/10.1038/nmeth765.

61. Livak KJ, Schmittgen TD. 2001. Analysis of relative gene expression data using real-time quantitative PCR and the $2^{-\Delta\Delta CT}$ method. Methods 25:402–408. https://doi.org/10.1006/meth.2001.1262.

62. Quinn JD, Weening EH, Miner TA, Miller VL. 2019. Temperature control of *psaA* expression by PsaE and PsaF in *Yersinia pestis*. J Bacteriol 201:e00217-19. https://doi.org/10.1128/JB.00217-19.